Egypt. J. Chem. **Vol. 65**, No. 5 pp. 221 – 230 (2022)

Egyptian Journal of Chemistry

http://ejchem.journals.ekb.eg/

Photocatalytic Degradation of Organic Dyes Using Lafeo$_3$hollow Fibres Prepared By Template Method

M.M.Samy[1],A.H. Zaki[2]* ,A. A.Farghali[2], M. M. EL-Deeb[1]

[1]*Chemistry Department, Faculty of Science, Beni-Suef University, Beni-Suef, Egypt.*

[2]*Materials Science and Nanotechnology Department, Faculty of Postgraduate Studies for Advanced Sciences, Beni-Suef University, Egypt*

Abstract

Perovskite $LaFeO_3$ hollow fibers with porous walls have been synthesized using cotton as biotemplates and lanthanum nitrate and ferric nitrate solution as precursors and then sintered in air at different temperatures. Effect of calcination temperature on the catalytic and photocatalytic activity of $LaFeO_3$ hollow fibers towards the degradation of methylene blue dye was studied. Samples were characterized by X-ray powder diffraction (XRD), Transmission electron microscope (TEM), Scanning electron microscope (SEM) Brunauer–Emmett–Teller (BET), photoluminescence spectrum (PL), Zeta potential, and UV-Vis spectroscopyanalysis. XRD, SEM, and TEM proved the successful synthesis of perovskite $LaFeO_3$ hollow fibers with crystalline size from 19.9 nm to 41nm. It is found that by increasing calcination temperature, the catalytic and photocatalytic activity of $LaFeO_3$ hollow fibers increased.

Keywords :Perovskite, fibers, LaFeO3, photocatalytic activity.

1. Introduction

Due to the fast creation of industrial cultures, the level of people's life is going up quickly. In the meantime, the detrimental effect of humans on the environment is so dangerous. Thus, in the past ten years, the removal of organic or inorganic pollutants from wastewater by degradation has revealed extensive interest.[1–4] To overcome this problem, many attempts have been adopted to handle these contaminants, like biotechnology,[5,6] physical treatment for wastewater,[7] physical adsorption, [8, 9], and so forth. these approaches are not only of poor efficiency but also expensive. Semiconductor photocatalysis based on using and converting solar energy into chemical energy has been planned to be a green and favourable way to solve energy shortage problems and environmental challenges.[10–14] In the last few decades, titanium dioxide(TiO_2) as an n-type semiconductor has attracted wide concern as a photocatalyst, as it is available, cheap, safe, highly active, and photochemical stable.[15] But, they found that titanium dioxide(TiO_2) can absorb only the ultraviolet (UV) light which represents a small portion (<6%) of the solar energy because of its large band gap of (3.0–3.2eV), which restricts its practical photocatalytic applications.[16]Perovskite-type oxide semiconductors have attracted extensive interest for using as photocatalysts to get rid of harmful organic compounds by degradation. Perovskite-type oxides have a general formula of ABO3, where A represents the rare-earth ion and B represents the transition metal ion. The activity of Perovskite Lanthanum orthoferrite (LaFeO3) nanocrystals under visible light has attracted extensive interest to be used in

*Corresponding author e-mail: ayman.zaki@psas.bsu.edu.eg
Receive Date: 27 September 2021, Revise Date: 03 November 2021, Accept Date: 16 November 2021
DOI: 10.21608/ejchem.2021.98283.4578

progressing applications like oxide fuel cells[17], photocatalysts[18-21], and gas sensors[22].The visible-light photocatalytic behavior of $LaFeO_3$ depends mainly on the structure, morphology, and size of the catalyst, which is specified according to the synthesis method. A lot of studies have been interested in the preparation of LaFeO3 powders[23,24], nanowires[25], and thin films[26], but few papers have concentrated on the synthesis and structural properties of LaFeO3 hollow fibers. It is found that controlled synthesis of homogeneous, high-purity and high surface area $LaFeO_3$ semiconductors is vital to get numerous properties [27] for more applications. In this work, we choose cotton as a biotemplate because it has low cost and it is a green source to prepare $LaFeO_3$ hollow fibers with high surface area and high visible-light photocatalytic activity. The photocatalytic activity of $LaFeO_3$ hollow fibers calcinated at different temperatures in the decomposition of methylene blue (MB) aqueous solution under visible light was studied.

2. Experimental procedure

Materials

Lanthanum nitrate La $(NO_3)_3 \cdot 6H_2O$ and ferric nitrate $Fe(NO_3)_3 \cdot 9H_2O$ were obtained from Sigma Aldrich Company(Germany). Absorbent medical cotton from chemical and medical instruments company(Egypt).

Procedure

Lanthanum nitrate ($La(NO_3)_3 \cdot 6H_2O$) and ferric nitrate ($Fe(NO_3)_3 \cdot 9H_2O$) were used as startingmaterials. 0.43301 gm of $La(NO_3)_3.6H_2O$ and 0.404 gm of $Fe(NO_3)$, $3.9H_2O$ were first dissolved in 10 ml of distilled water and stirred with a magnetic stirrer at (330 rpm) for half an hour. Then, 1 gm of dried and loose cotton fibres were penetrated with the solution above. After drying at 80° C for 22 hour, it was then placed in a crucible, and burnt in the air at 600° C, 700° C, 800° C, and 900° C for 3 hr, respectively. Due to this sintering technique, the cotton templates were eliminated, and $LaFeO_3$ hollow fibres were synthesized, finally, the product was grinded with mortar to get fine fibres.[22]

3. characterization

XRD analysis

By an X-ray powder diffraction (XRD) patterns using Cu Kα radiation with wavelength 0.154 cm^{-1} at voltage of acceleration 40 kV, a scan angle range of 5−80°,a current of 35 mA, and a scan step of 0.02°at faculty of postgraduate studies for advanced science, The crystalline phase in the samples was characterized.

Morphological analysis

Morphological properties of samples were studied by scanning electron microscopy (SEM Model Quanta 250 FEG) MEITECH K550X sputter coater made in England at housing and building national research centre. The high-resolution transmission electron microscopy (HR-TEM) images were obtained using FEI Tecnai (G2 F20) operating at 200 kV at the Egyptian petroleum research institute.

Photoluminescence (PL)spectroscopy

Spectrofluorometer was used to obtain Photoluminescence(PL) spectroscopy, Model Jasco FP-6500, made in Japan and Light source was Xenon arc lamp 150 watt) at the national research centre.

BET surface area and Zeta potential

Micromeritics ASAP 2010M+C system at the Egyptian petroleum research institute was used for The adsorption and desorption isotherm studies with liquid nitrogen. A single point Brunauer–Emmett–Teller (BET) method was used to investigate the precise surface area. Pore size distribution was measured from the isotherm of nitrogen adsorption, using (Barrett–Joyner–Halenda) method. The Brunauer-Emmett-Teller (BET) surface areas were estimated from nitrogen adsorption-desorption isotherms technique at the Egyptian petroleum research institute. All the samples were degassed at 150^{o} C overnight prior to the adsorption measurements.

Zeta potential was measured for all samples using A Zetasizer 2000 analyzer (Malvern Co., UK) at the faculty of postgraduate studies for advanced science.

4. Photocatalytic activity testing

The photocatalytic activity of the $LaFeO_3$ calcinated at different temperatures (600^o C, 700^o C, 800^o C, and 900^o C)was estimated by measuring the photocatalytic degradation of MB alone and with four samples at room temperature under solar-simulated light Sol 1A (a xenon reactor equipped with a cooling system with 150 watt power) at a wavelength of 300−800 nm at neutral pH 7 .

The experiments were performed by adding (50mg) $LaFeO_3$ to a 20 mL (2ppm) MB aqueous solution, and before illumination, each suspension was stirred using magnetic stirrer in the dark for 90 min to get the adsorption-desorption equilibrium, followed by exposing to visible-light irradiation. After a specified time interval (each 15mint) during the visible-light irradiation, the suspension was centrifuged at 10000 rpm for 2 min, and the top clear solution was measured in the range 400-800 nm using the UV-visible absorption spectrophotometer. The residual MB concentration was measured by absorbance at 665 nm [18].

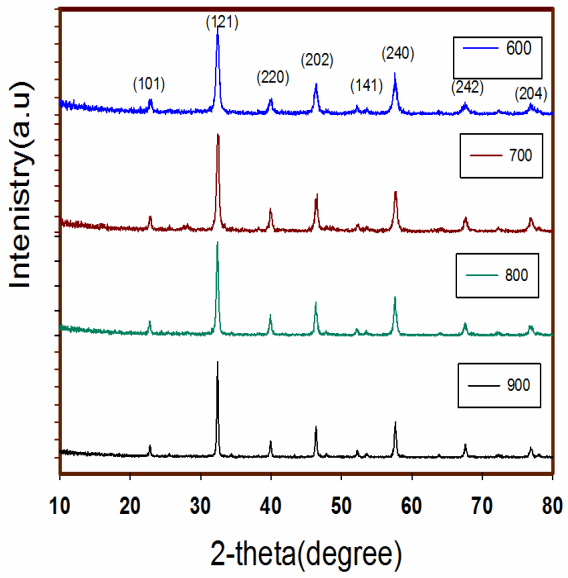

Fig. 1 X-ray diffraction patterns of La FeO_3 at different calcination temperatures

5. Results and discussion

Fig.(1)shows the crystalline phases of the cotton-templated $LaFeO_3$ hollow fibres calcinated at 600^o C, 700^o C, 800^o C, and 900^o C obtained from XRD analysis. It can be observed that all samples have displayed the same diffraction peaks around 2θ= 22.6°, 32.14°, 39.7°, 46.06°,52.2°, 57.5°,67.4°,76.5^o correspond to the characteristic crystal planes (101), (121), (220), (202), (141), (240), (242) and (204) of orthorhombic $LaFeO_3$ perovskite (JCPDS file no. 37–1493)[28], and no other peaks were detected.

Also, there are no carbonaceous materials peaks were detected which confirms the complete combustion and removal of the used cotton.[22] Results revealed that by increasing annealing temperature the XRD peaks become narrower and more intense referring to improvement in crystallization, and increasing crystallite size. The mean crystallite size for different calcination temperatures LaFeO3(D) have been estimated by using the Debye-Scherer equation:[29]

$D = K\lambda / (\beta \cos\theta)$

Where K is the factor of crystallite shape, λ the wavelength of X-ray, θ is the diffraction angle and β is the diffraction peak width. The average crystallite size of LaFeO3 samples increased by increasing calcination temperature to be 19.9 nm, 26.7nm, 30.2nm, and 41nm for 600^o C, 700^o C, 800^o C, and 900^o C respectively. Figure(2) and (4) displays the SEM images of the as-prepared hollow fibres calcinated at 700^o C and 800^o C. These fibres have the same morphology of the original cotton fibres template, with the removal of the cotton tissues. As seen in fig(2) and (4) the $LaFeO_3$ fibres are hollow, long, and have an inner diameter of about 4.2 μm. Fig(3) and (5) shows the high magnification SEM images of single biomorphic $LaFeO_3$ fibres calcinated at 700^o C and 800^o C . These fibres are hollow and their walls consist of numerous amounts of interconnected $LaFeO_3$ nanoparticles with a number of pores between them. That proved the porosity of the walls of $LaFeO_3$ hollow fibres so that the reactants can diffuse into the catalyst easily. It is clear also that morphology didn't change by increasing calcination temperature.

The microstructure of $LaFeO_3$ hollow fibers calcinated at 700^o C. has been checked by TEM and HRTEM. As shown in fig.(6) and (7) fibers consist of many $LaFeO_3$ grains with a grain size of 25-33 nm, which confirms the XRD results.

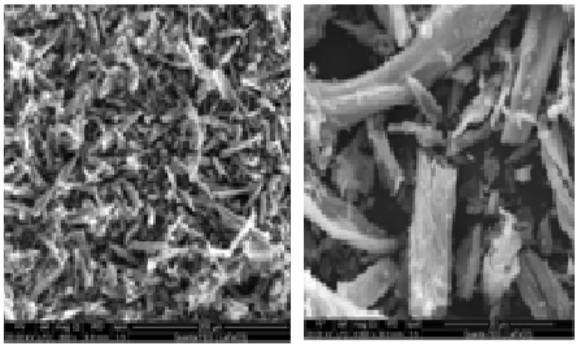

Fig.2SEM images of $LaFeO_3$ hollow fiberssintered at 700° C with different magnifications.

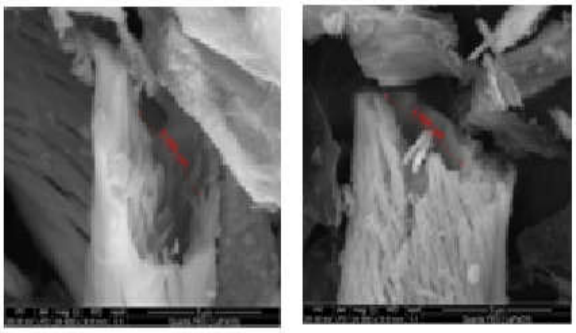

Fig.3 Highly magnified SEM images of biomorphic $LaFeO_3$ hollow fiber calcinated at 700° C.

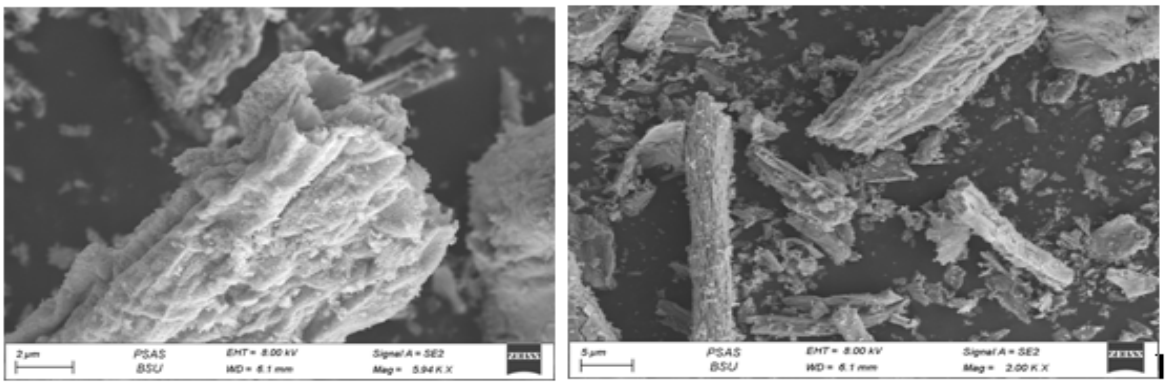

Fig.4SEM images of LaFeO3 hollow fibers sintered at 800° C with different magnifications.

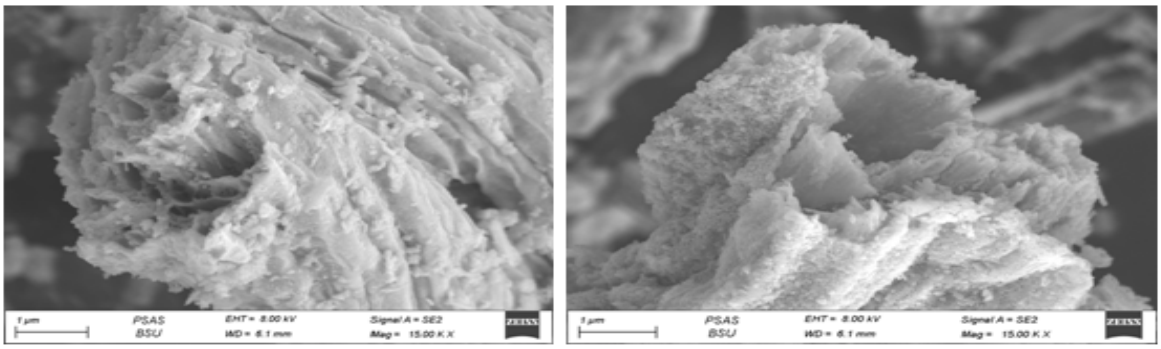

Fig.5 Highly magnified SEM images of biomorphic $LaFeO_3$ hollow fibers calcinated at 800° C.

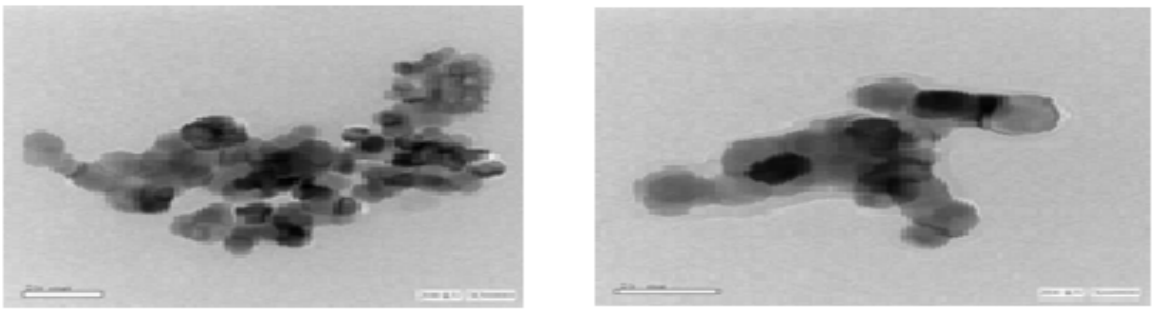

Fig.6 TEM images of the $LaFeO_3$ hollow fibers calcinated at 700° c nanofibers.

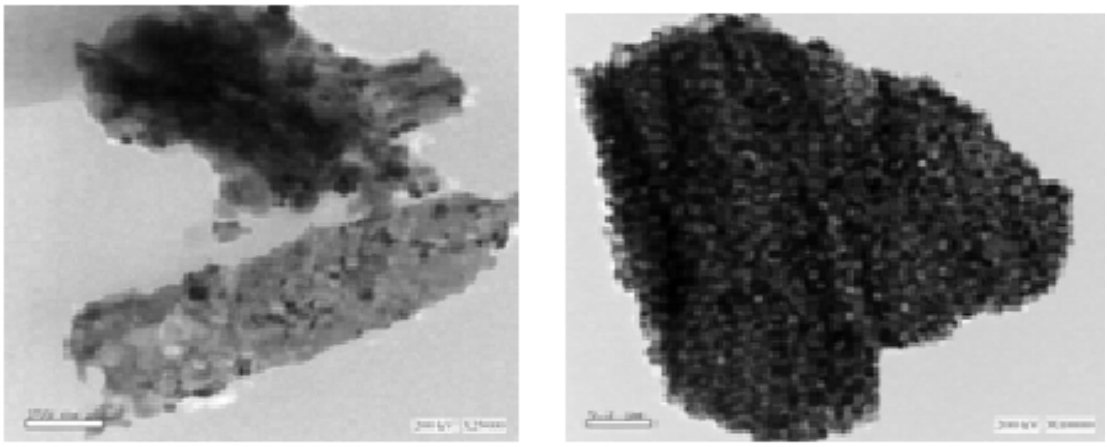

Fig.7 HRTEM images of the $LaFeO_3$ hollow fibers calcinated at 700^o C nanofibers

Fig. (8) represents nitrogen adsorption-desorption isotherms of cotton-templated $LaFeO_3$ hollow fibres calcinated at 600^o C, 700^{o}C, 800^o C, and 900^{o}C. According to the International Union of Pure and Applied Chemistry classification, the isotherms in Fig.8 are classified into type-IV nature. Based on the type of isotherms, all samples can be considered as mesoporous $LaFeO_3$ hollow fibres. Because of the capillary condensation within the pores phenomenon, the formation of hysteresis loops in the isotherms was noticed in all samples.[30] The porosity of samples confirms SEM results. As seen in table1 by increasing calcination temperature, the average pore size diameter increases from 27.25nm for 600^o C sample to 44.19 nm for 900^{o}C sample. It can be also observed in a table (1) that the BET surface areas of $LaFeO_3$ hollow fibbers decrease by increasing calcination temperature to be 19.6, 10.4, 9.3, and 7.01 m2/g for 600^{o}C, 700^{o}C, 800^o C, and 900^o C samples respectively. This agrees with the crystallite size variation in XRD results.

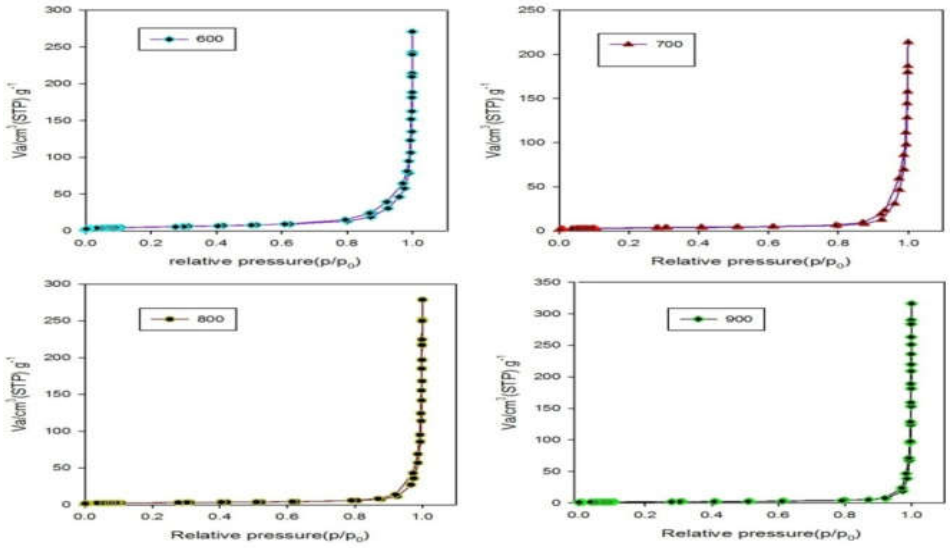

Fig.8 N2 adsorption-desorption isotherms for $LaFeO_3$ hollow fibers calcinated at different temperatures

Table.1crystallite size, surface area, pore-volume, and pore diameter for $LaFeO_3$ hollow fibers calcinated at different temperature

LaFeO3 hollow fibbers	Crystallite Size [nm]	$a_{s(BET)}[m^2 g^{-1}]$	Total pore volume[cm^3g^{-1}]	Mean pore diameter[nm]
600° c	**19.9**	**19.6**	**0.13**	**27.25**
700° c	**26.7**	**10.4**	**0.12**	**47.45**
800° c	**30.2**	**9.3**	**0.11**	**45.26**
900° c	**41.0**	**7.01**	**0.08**	**44.19**

Table2 shows the Zeta potential value of $LaFeO_3$ hollow fibres calcinated at different temperatures. The Zeta potential increased From (-7.22 to -1.70) when calcination temperature increased from 600° C to 900° C. This indicated that by increasing calcinations temperature, the surface potential increased, and its adsorption capacity towards cationic dye such as MB increased also. Identically, other adsorbents including Beta zeolite [31], GO-zeolite [32], and wheat straw [33] had also the same negative surface potential.

Table2 zeta potential values for $LaFeO_3$ hollow fibers calcinated at different temperatures

LaFeO3 hollow fibers	600° c	700° c	800° c	900° c
Zeta potential(mv)	-7.22	-6.26	-3.63	-1.70

The PL spectroscopy is a valuable method for studying the optical, electric structure, and photoelectric properties of semiconductor nanomaterials. Fig.9 displays the photoluminescence spectra of $LaFeO_3$ hollow fibres calcinated at

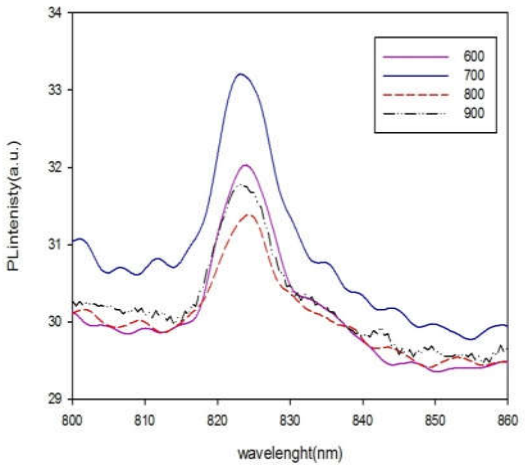

Fig.9 PL spectra of $LaFeO_3$ hollow fibers calcinated at different temperatures

different temperatures with an excitation wavelength of 750 nm. All samples show clear PL signals at the wavelength range from 800 to 860 nm . all $LaFeO_3$ fibres samples display the main PL signal at wavelength 825nm. Electronic transitions from the conduction band to the valence band are basically responsible for these PL signals (band-band PL)[34]. It can be seen in fig.9 that by increasing calcination temperature, the PL spectrum intensity decreases. From XRD result by increasing calcination temperature, the crystallite size increase so

crystallinity of $LaFeO_3$ hollow fibres increases, the separation rate of photo-induced charge carriers increases and so photocatalytic activity increases According to the band–band PL spectrum of semiconductor materials. [35] these results display that 800° Cand 900° Csamples have the same photocatalytic activity more than 600° Cand 700° Csamples.

Photocatalytic activities

The photocatalytic activity of $LaFeO_3$ hollow fibres calcinated at different temperatures was estimated by decomposition of MB dye solution under visible light irradiation. Fig(10) illustrates the rate of MB degradation of the photocatalytic reaction under visible light and adsorption in dark using $LaFeO_3$ hollow fibres calcinated at different temperatures as a catalyst. As known that MB shows good stability in the dark and under visible light as shown in fig(10).[36] Results show that for all samples by photocatalytic activities due to the presence of extra routes of holes trapping which increase the separation rate of electron-hole pairs.[37]It can be observed that by increasing calcinating temperature, the catalytic and photocatalytic activity of $LaFeO_3$ hollow fibres gradually increases to reach to total MB removal of 45%, 51%, 79% and 78 % for 600° C, 700° C, 800° C, and 900° C samples respectively, so samples calcinating at 800° C and 900° C show the best photocatalytic activity. It could be due to that, by increasing calcinating temperature the crystallinity of $LaFeO_3$ hollow fibres increases which nourishes the photoinduced charge separation[38]and these results confirm PL results, also increasing the adsorbed O_2 on the $LaFeO_3$ surface promotes superoxide radicals. [39]It can be also observed that increasing temperature after 800° C did not show a significant difference. When $LaFeO_3$hollow fibres were exposed to visible light illumination with photon energy equal to or greater than the energy of band gap, holes, and electrons were found in valence and conduction bands. The excited electron was transported to the $LaFeO_3$ surface, where it reacted with adsorbed $O_2$and OH^-/H_2O to form $O_2^{\bullet -}$ and $^{\bullet}OH$ radicals. These radicals participated in the degradation of MB molecules into CO_2 and H_2O. The reaction mechanism is occurring as follows:[38]

increasing adsorption time, the MB concentration decreases till reaches equilibrium within 90mint for all samples, because of MB adsorption on their surfaces. Equilibrium value for MB adsorption with 600° C, 700° C, 800° C, and 900° C samples was 15%, 20%, 63%, and 62 % respectively, so the adsorption capacity for samples increases by increasing calcinating temperature, due to increasing the surface potential which confirms Zeta potential results. After that, the effect of visible light irradiation on photocatalytic degradation of MB (2ppm) using $LaFeO_3$ hollow fibres calcinated at different temperatures was studied during 135 min. The visible-light absorption of $LaFeO_3$ hollow fibres is basically responsible for its visible-light photocatalytic activity. In particular, visible-light irradiation can excite $LaFeO_3$, resulting in effective electron-hole pair separation, which participates in the oxidation decomposition of MB.[36]Perovskite oxides, that own great lattice distortion, have high

$$LaFeO_3 + h\nu \longrightarrow LaFeO_3 + e^-_{CB} + h^+_{VB} \quad [1]$$

$$e^-_{CB} + O_2O_2^{\bullet -} \longrightarrow \quad [2]$$

$$O_2^{\bullet -} + H_2O \longrightarrow HO_2^{\bullet} + OH \quad [3]$$

$$HO_2^{\bullet} + H_2O \longrightarrow H_2O_2 + OH^{\bullet} \quad [4]$$

$$H_2O_2{}^{\bullet}2OH^{\bullet} \longrightarrow \quad \textbf{[5]}$$

$$h^+ + OH^- \longrightarrow OH^{\bullet} \quad \textbf{[6]}$$

$$OH^{\bullet} + MB(dye) \longrightarrow CO_2 + H_2O \quad [7]$$

$$h^+ + MB(dye) \longrightarrow CO_2 + H_2O \quad \textbf{[8]}$$

$$e^-_{CB} + h^+_{VB} \longrightarrow h\nu + \text{recombination} \quad [9]$$

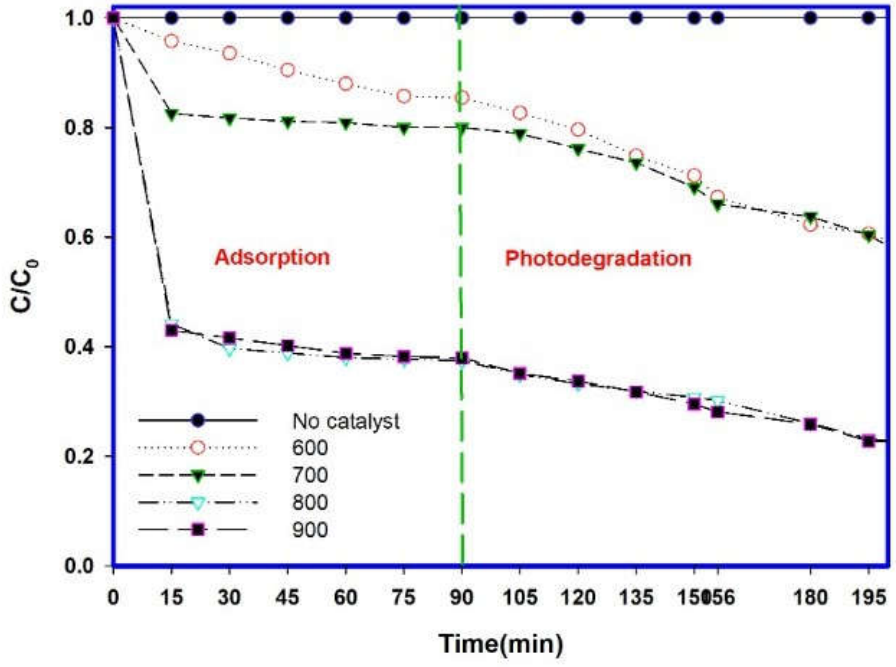

Fig 10. MB adsorption and Photocatalytic activity of $LaFeO_3$ hollow fibers calcinated at different temperatures.

6. Conclusions

In conclusion, we have synthesized orthorhombic perovskite $LaFeO_3$ hollow fibbers by an easy and cheap method using cotton as a template. Comparison has been made between samples calcinated in the air at four different temperatures. XRD data proved that all samples have an orthorhombic structure with a single-phase, and The average crystallite size of $LaFeO_3$ samples increased by increasing calcination temperature to be 19.9 nm, 26.7nm, 30.2nm, and 41nm for 600^o C, 700^o C, 800^o C, and 900^o C respectively. SEM images demonstrated the successful synthesis of $LaFeO_3$ hollow fibres with porous walls, which promotes the active surface area. It is found that by increasing calcinating temperature, catalytic and photocatalytic activity increases. Sample calcinated at 800^o C considered to have the best catalytic and photocatalytic activity due to the best crystallinity of it which promotes the photoinduced charge separation and these results confirm PL results, also increasing the adsorbed O_2 on the $LaFeO_3$ surface promotes superoxide radicals, But it is noticed that raising temperature more than this degree doesn't have a great effect on activity.

7. Conflicts of interest

All authors declare that they have no conflict of interest.

8. Acknowledgment

This work was supported by StamatisDouzinas scholarship from titan cement Egypt (annual scholarship program for graduates from Beni suef and Alex.) to keep up with post-graduate studies.

9. References

[1] Wen, X. J., Niu, C. G., Zhang, L., Liang, C., Guo, H., & Zeng, G. M. (2018). Photocatalytic degradation of ciprofloxacin by a novel Z-scheme CeO2–Ag/AgBrphotocatalyst: Influencing factors, possible degradation pathways, and mechanism insight. Journal of catalysis, 358, 141-154.

[2]Taghavi, M., Ehrampoush, M. H., Ghaneian, M. T., Tabatabaee, M., &Fakhri, Y. (2018). Application of a Keggin-type heteropoly acid on supporting nanoparticles in photocatalytic degradation of organic

pollutants in aqueous solutions. Journal of Cleaner Production, 197, 1447-1453.
[3] Pandey, P., Shinde, V. N., Deopurkar, R. L., Kale, S. P., Patil, S. A., & Pant, D. (2016). Recent advances in the use of different substrates in microbial fuel cells toward wastewater treatment and simultaneous energy recovery. Applied Energy, 168, 706-723.
[4] Li, Q., Qian, J., Du, L., & Zhao, Q. (2020). Zinc-tetracarboxylate framework material with nano-cages and one-dimensional channels for excellent selective and effective adsorption of methyl blue dye. RSC Advances, 10(6), 3539-3543.
[5] Qi, W., Zhang, H., Liu, R., Liu, H., &Qu, J. (2019). Effects of different secondary biological treatment processes followed by flocculation and sand-filtration on subsequent DBPs control from sewage treatment plants. Separation and Purification Technology, 211, 81-89.
[6] Perini, J. A. L., Tonetti, A. L., Vidal, C., Montagner, C. C., &Nogueira, R. F. P. (2018). Simultaneous degradation of ciprofloxacin, amoxicillin, sulfathiazole and sulfamethazine, and disinfection of hospital effluent after biological treatment via photo-Fenton process under ultraviolet germicidal irradiation. Applied Catalysis B: Environmental, 224, 761-771.
[7] Kumar, P., Bansal, V., Kim, K. H., & Kwon, E. E. (2018). Metal-organic frameworks (MOFs) as futuristic options for wastewater treatment. Journal of industrial and engineering chemistry, 62, 130-145.
[8] Holt, A. P., Bocharova, V., Cheng, S., Kisliuk, A. M., White, B. T., Saito, T., ...&Sokolov, A. P. (2016). Controlling interfacial dynamics: covalent bonding versus physical adsorption in polymer nanocomposites. ACS nano, 10(7), 6843-6852.
[9]Xie, H., Chen, Q., Chen, J., Chen, C. E. L., & Du, J. (2018). Investigation and application of diffusive gradients in thin-films technique for measuring endocrine disrupting chemicals in seawaters. Chemosphere, 200, 351-357.
[10]Fujishima, A., & Honda, K. (1972). Electrochemical photolysis of water at a semiconductor electrode. nature, 238(5358), 37-38.
[11] Hoffmann, M. R., & ST Martin, W. Y. (1995). Choi, and DW. Bahnemann,"Environmental Applications of Semiconductor Photocatalysis,". Chem Rev, 95(1), 69-96.
[12]Neppolian, B., Kim, Y., Ashokkumar, M., Yamashita, H., & Choi, H. (2010). Preparation and properties of visible light responsive ZrTiO4/Bi2O3 photocatalysts for 4-chlorophenol decomposition. Journal of hazardous materials, 182(1-3), 557-562.
[13] Long, R., & English, N. J. (2009). Synergistic effects of Bi/S codoping on visible light-activated anatase TiO2 photocatalysts from first principles. The Journal of Physical Chemistry C, 113(19), 8373-8377.
[14] Inoue, T., Fujishima, A., Konishi, S., & Honda, K. (1979). Photoelectrocatalytic reduction of carbon dioxide in aqueous suspensions of semiconductor powders. Nature, 277(5698), 637-638.
[15] Ng, Y. H., Lightcap, I. V., Goodwin, K., Matsumura, M., &Kamat, P. V. (2010). To what extent do graphene scaffolds improve the photovoltaic and photocatalytic response of TiO2 nanostructured films?. The Journal of Physical Chemistry Letters, 1(15), 2222-2227.
[16] Sakthivel, S., &Kisch, H. (2003). Daylight photocatalysis by carbon□modified titanium dioxide. AngewandteChemie International Edition, 42(40), 4908-4911.
[17] Liu, L., Sun, K., Li, X., Zhang, M., Liu, Y., Zhang, N., & Zhou, X. (2012). A novel doped CeO2–LaFeO3 composite oxide as both anode and cathode for solid oxide fuel cells. international journal of hydrogen energy, 37(17), 12574-12579.
[18] Tang, P., Tong, Y., Chen, H., Cao, F., & Pan, G. (2013). Microwave-assisted synthesis of nanoparticulateperovskite LaFeO3 as a high active visible-light photocatalyst. Current Applied Physics, 13(2), 340-343.
[19] Zhang, Q., Huang, Y., Peng, S., Zhang, Y., Shen, Z., Cao, J. J., ...&Pui, D. Y. (2017). Perovskite LaFeO3-SrTiO3 composite for synergistically enhanced NO removal under visible light excitation. Applied Catalysis B: Environmental, 204, 346-357.
[20] Zhu, J., Li, H., Zhong, L., Xiao, P., Xu, X., Yang, X., ...& Li, J. (2014). Perovskite oxides: preparation, characterizations, and applications in heterogeneous catalysis. Acs Catalysis, 4(9), 2917-2940.
[21] Zhu, J., Zhao, Y., Tang, D., Zhao, Z., &Carabineiro, S. A. (2016). Aerobic selective oxidation of alcohols using La1− xCexCoO3 perovskite catalysts. Journal of Catalysis, 340, 41-48.
[22] Song, P., Wang, Q., Zhang, Z., & Yang, Z. (2010). Synthesis and gas sensing properties of

biomorphic LaFeO3 hollow fiberstemplated from cotton. Sensors and Actuators B: Chemical, 147(1), 248-254.
[23] Berchmans, L. J., Sindhu, R., Angappan, S., & Augustin, C. O. (2008). Effect of antimony substitution on structural and electrical properties of LaFeO3. journal of materials processing technology, 207(1-3), 301-306.
[24] Qi, X., Zhou, J., Yue, Z., Gui, Z., & Li, L. (2003). A simple way to prepare nanosized LaFeO3 powders at room temperature. Ceramics international, 29(3), 347-349.
[25] Yang, Z., Huang, Y., Dong, B., & Li, H. L. (2006). Controlled synthesis of highly ordered LaFeO3 nanowires using a citrate-based sol–gel route. Materials research bulletin, 41(2), 274-281.
[26] Lee, Y. H., & Wu, J. M. (2004). Epitaxial growth of LaFeO3 thin films by RF magnetron sputtering. Journal of crystal growth, 263(1-4), 436-441.
[27] Yang, Z., Huang, Y., Dong, B., & Li, H. L. (2005). Fabrication and structural properties of LaFeO 3 nanowires by an ethanol–ammonia-based sol–gel template route. Applied Physics A, 81(3), 453-457.
[28] Liang, Q., Jin, J., Liu, C., Xu, S., & Li, Z. (2017). Constructing a novel pnheterojunctionphotocatalyst LaFeO3/g-C3N4 with enhanced visible-light-driven photocatalytic activity. Journal of Alloys and Compounds, 709, 542-548.
[29] Ju, L., Chen, Z., Fang, L., Dong, W., Zheng, F., &Shen, M. (2011). Sol–gel synthesis and photo□Fenton- like catalytic activity of EuFeO3 nanoparticles. Journal of the American Ceramic Society, 94(10), 3418-3424.
[30] Wu, Z., Wang, L., Hu, Y., Han, H., Li, X., & Wang, Y. (2020). The preparation, characterization, and catalytic performance of porous fibrous LaFeO 3 perovskite made from a sunflower seed shell template. Frontiers of Chemical Science and Engineering, 14, 967-975.
[31] Liang, X., Zhang, Y., Qu, Y., Han, Y., Wang, X., Cheng, A., ...& Zhao, L. (2018). Synthesis of HKUST-1 and zeolite beta composites for deep desulfurization of model gasoline. RSC advances, 8(25), 13750-13754.
[32] Yu, Y., Murthy, B. N., Shapter, J. G., Constantopoulos, K. T., Voelcker, N. H., & Ellis, A. V. (2013). Benzene carboxylic acid derivatizedgraphene oxide nanosheets on natural zeolites as effective adsorbents for cationic dye removal. Journal of hazardous materials, 260, 330-338.
[33] Xu, X., Gao, B. Y., Tan, X., Yue, Q. Y., Zhong, Q. Q., & Li, Q. (2011). Characteristics of amine-crosslinked wheat straw and its adsorption mechanisms for phosphate and chromium (VI) removal from aqueous solution. Carbohydrate Polymers, 84(3), 1054-1060.
[34] Li, K., Wang, D., Wu, F., Xie, T., & Li, T. (2000). Surface electronic states and photovoltage gas-sensitive characters of nanocrystalline LaFeO3. Materials chemistry and physics, 64(3), 269-272.
[35] Yu, J. G., Yu, H. G., Cheng, B., Zhao, X. J., Yu, J. C., &Ho, W. K. (2003). The effect of calcination temperature on the surface microstructure and photocatalytic activity of TiO2 thin films prepared by liquid phase deposition. The Journal of Physical Chemistry B, 107(50), 13871-13879.
[36] Tang, P. S., Fu, M. B., Chen, H. F., & Cao, F. (2011). Synthesis of nanocrystalline LaFeO3 by precipitation and its visible-light photocatalytic activity. In Materials Science Forum (Vol. 694, pp. 150-154). Trans Tech Publications Ltd.
[37] Wu, J. M., & Zhang, T. W. (2004). Photodegradation of rhodamine B in water assisted by titania films prepared through a novel procedure. Journal of Photochemistry and Photobiology A: Chemistry, 162(1), 171-177.
[38] Thirumalairajan, S., Girija, K., Hebalkar, N. Y., Mangalaraj, D., Viswanathan, C., &Ponpandian, N. (2013). Shape evolution of perovskiteLaFeO 3 nanostructures: a systematic investigation of growth mechanism, properties and morphology dependent photocatalytic activities. RSC advances, 3(20), 7549-7561.
[39] Wiranwetchayan, O., Promnopas, S., Phadungdhitidhada, S., Phuruangrat, A., Thongtem, T., Singjai, P., &Thongtem, S. (2019). Characterization of perovskite LaFeO3 synthesized by microwave plasma method for photocatalytic applications. Ceramics International, 45(4), 4802-4809.